A Mobile Propagation Measurement System

Robert T. Johnk [1], Peter Papazian, Paul McKenna, Nicholas DeMinco, Geoffrey Sanders, Heather Ottke

Institute for Telecommunication Sciences (NTIA/ITS)
325 Broadway
Boulder, Colorado USA 80305
[1] bjohnk@its.bldrdoc.gov

Abstract—**This paper describes a mobile-to-mobile propagation measurement system that is currently being developed at the Institute for Telecommunication Sciences under the sponsorship of the Office of Spectrum Measurement. This system uses a fixed transmitter truck and a moving receiver van to characterize radio-frequency channels of selected urban and rural environments. The transmitter and receiver architectures are described, and selected time- and frequency-domain measurement results are presented. The results obtained so far are very promising and demonstrate the versatility and effectiveness of this measurement system.**

I. Introduction

A mobile-to-mobile propagation measurement system is currently being developed at the Institute for Telecommunication Sciences (NTIA/ITS) under the sponsorship of the Office of Spectrum Management (NTIA/OSM). The system is a channel sounder and it is used to obtain propagation data at selected frequencies. This sophisticated system is the culmination of many years of research by ITS engineers and scientists [1]-[8]. The transmitter and receiver are deployed on two vehicles, and can be used in a wide variety of environments. In the present configuration, the transmitter truck is parked in a fixed location. Its antennas are deployed on tripods, and it transmits signals simultaneously on four separate channels. The receiver van is driven over a prescribed route while it obtains channel data. The system transmits and receives a binary phase-shift keyed (BPSK) signal that is modulated with a maximum-length, pseudorandom noise (PN) sequence. The transmitted and received sequences are cross-correlated at baseband to produce high-resolution time-domain waveforms that are used to analyze the channel propagation characteristics. These waveforms can be post-processed to yield useful parameters such as path loss and delay spread. In addition, the time-domain waveforms yield insight into multipath propagation effects, range, and location of reflectors. Both narrowband and broadband propagation parameters can be extracted. This system has the ability to measure propagation effects in both the time- and frequency-domains. In addition, it has the ability to acquire large amounts of data at frequent intervals, providing dense sets of propagation data, sampled at twice the maximum Doppler frequency. So far, this system has been deployed in a variety of environments ranging from dense urban canyons to rural country roads.

Fig. 1 (a) Transmitter truck (with transmitting antennas deployed). (b) Receiver van being readied for propagation measurements.

II. System Features

The mobile-to-mobile propagation measurement system is deployed in the truck and van combination shown in Fig. 1.

As shown in Fig. 2, the transmitting equipment is mounted on racks in the control room in the back of the ITS-designed Radio Spectrum Measurement System (RSMS) truck. The mobile-to-mobile propagation measurement system is operated from a fixed location with the transmit antennas mounted on tripods at a nominal height of 1.5 m. Electrical power is supplied by either external shore power or with an internal 5 kW generator. A well-designed climate control system provides both heat and air conditioning to ensure all-season and all-weather operation.

The receiving equipment is rack-mounted in a modified cargo van. The van has a custom-installed, on-board generator that supplies 5 kW of power to ensure full mobile operation. The van is driven in prescribed patterns, and data are acquired at user-selected intervals and rates. Data can be acquired while the van is either stationary or in motion. On-board GPS and dead-reckoning tracking systems are used to generate precise position information while driving the routes.

Fig. 2. Interior view of the transmitter equipment rack.

The mobile-to-mobile propagation measurement system operates at selected channels in the frequency range of 183 to 5750 MHz. Bandwidths vary from 4 to 20 MHz—the narrower bandwidths are used to avoid potential interference with nearby services. Seven channels are available: 183 MHz (BW=4 MHz), 430 MHz (BW=20 MHz), 915 MHz (BW=20 MHz), 1350 MHz (BW=20 MHz), 1602.5 MHz (BW=10 MHz), 2260 MHz (BW=20 MHz), and 5750 MHz (BW=20 MHz).

The BPSK signals are transmitted with 511-bit maximum-length PN sequences that have chip rates of 2 Mbps, 5 Mbps, and 10 Mbps, with bandwidths of 4 MHz, 10 MHz, and 20 MHz, respectively. The system is designed to transmit at variable chip rates to avoid disruption of existing radio services. The resulting signal has a noise-like character with a reduced interference potential. The total transmitted EIRP levels vary from 10 to 30 W.

The transmitter and receiver are phase-synchronized using high-precision 10 MHz rubidium clocks calibrated to the National Institute of Standards and Technology (NIST) atomic clock. The received BSPK signals are down converted to a 10-MHz intermediate frequency (IF) using analog hardware, and then digitized using a high-speed data acquisition system.

The received data are cross-correlated with the known transmitted sequence (post-processing) to generate time-domain channel impulse responses with range resolutions that vary from 30 to 150 m, depending on the channel bandwidth.

The ability to generate high-fidelity waveforms with variable chip rates is unique. Indeed, it provides a powerful tool that greatly facilitates the study of propagation effects. We can now assess such parameters as range (time-delay), and get a direct view of the multi-path scattering. In some cases, we can identify the source of the scattering (e.g., buildings, hills, power lines). The waveforms can be used to compute useful channel parameters such as the root mean squared (RMS) delay spread at any of the receiver locations. We can also investigate frequency-domain effects or parameters such as path loss (basic and excess), and both narrowband and broadband fading effects.

Table I
CHANNEL GROUPING, FREQUENCIES, CHIP RATES, AND BANDWIDTHS.

Group	Channel Number	Frequency (MHz)	Chip Rate Mbps	Bandwidth (MHz)
1	1	430	10	20
	2	1350	10	20
	3	2260	10	20
	4	5750	10	20
2	1	183	2	4
	2	915	10	20
	3	1602.5	5	10
	4	5750	10	20

III. TRANSMITTER

The transmitter is implemented using a combination of commercial off-the-shelf (COTS) components, as well as components designed and fabricated by ITS. The transmitter is designed to operate on seven different channels, but only four can be used at once. The channels are divided into the two groups shown in Table I: group 1: 430 MHz, 1350 MHz, 2260 MHz, and 5750 MHz, and group 2: 183 MHz, 915 MHz, 1602.5 MHz, and 5750 MHz. The 5750-MHz channel is used with each configuration as a check on measurement repeatability. Each of the group 1 channels is modulated at 10-Mbps chip rate resulting in channel bandwidth of 20 MHz. The group 2 channels, on the other hand, are transmitted at different chip rates: 183 MHz (2 Mbps), 915 MHz (10 Mbps), 1602.5 MHz (5 Mbps). The signals are generated using a combination of a variable chip rate generator, signal generators, and analog radio frequency (RF) hardware.

The PN codes are generated with a commercially-available programmable waveform generator. The generator is programmed to produce three separate 511-bit baseband PN sequences at chip rates of 10 Mbps, 5 Mbps, and 2 Mbps. The resulting sequences have peak voltages of ±0.5 V. The generator has a stored 511-bit PN sequence and plays it back at the different chip rates. The 10 Mbps PN sequence repeats at an interval of 51.1 μs, the 5 Mbps at 102.2 μs, and the 2 Mbps at 255.5 μs. The sequences are then low-pass filtered at bandwidths corresponding to the chip rates (e.g., $f_{lp} = 2$ MHz

Fig. 3. Group 2 transmitting antennas deployed at a rural site.

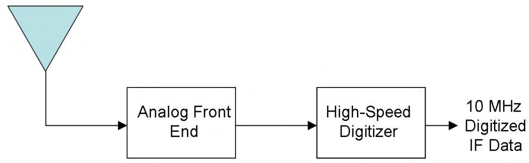

Fig. 4. Receiver system architecture

for 2 Mbps). Next, the sequences are input to a mixer, and up-converted to the desired RF frequency.

A synthesized generator, which is synchronized to a rubidium clock, provides the local oscillator drive. The mixer output power levels then are boosted with two stages of amplification, using a power amplifier as the output stage. Attenuators are distributed throughout the system to ensure good impedance matching, and to provide a gain balance that minimizes nonlinear distortion and interference potential. The power amplifier outputs are directly connected to the antenna inputs for signal transmission into the environment.

The transmit antennas are deployed at a nominal height of 1.5 m to simulate a mobile-to-mobile wireless scenario. (see Fig. 3). COTS collinear dipole arrays are used on six of the channels, and a COTS discone antenna is used on the remaining 183-MHz channel. A discone was used due to the lack of availability of collinear dipoles in this frequency range. The antennas are placed 3 to 4 m away from the truck, and are positioned to minimize blockage effects.

The antennas can be readily switched from the group 1 to the group 2 configuration. Switching from transmit configuration 1 to 2 involves changing out three antennas, changing the transmit cables, adjusting amplifier settings, performing transmitted power measurements, performing spectrum analyzer checks of the transmitted signal, and changing out filters and attenuators. All in all, this process takes about 20 minutes.

IV. Receiver

The receiver, shown in Fig. 4, consists of two main parts, an analog front-end and a high-speed digitizer.

The receiver is configured from both COTS and ITS-engineered systems. The purpose of the analog front-end is to down convert the RF signal to a 10-MHz IF signal, which is fed into a high-speed digitizer. The digitized data is then post-processed to extract the propagation parameters of interest.

Figure 5. Interior view of the receiver mounted in the van.

The receiver employs a dual-conversion architecture. The signals from the antennas are bandpass filtered, amplified and fed to the first mixer. The signals are then down converted to the first IF frequency of 150 MHz, where additional amplification and filtering are applied. The signals are then down converted to a 10-MHz IF signal. The second IF is filtered and amplified and fed to the inputs of a high-speed digitizer. Attenuators are used throughout the receiver chain to provide impedance matching at the mixer inputs, and to balance the gain characteristics of each channel—this maximizes dynamic range and ensures linearity.

The receiver has a fixed gain and it does not have an automatic gain control (AGC), which could filter out signal variations and bias the data. As a result, the system is deployed in a high-power mode for a distance of 100 m or greater, and a low-power mode (with power amplifiers removed) for transmit and receive antenna separations of 100 m or less. This approach is used to avoid saturating the receiver, which frequently occurs at closer distances.

Commercially-available frequency synthesizers are used as local oscillator sources. Separate sets of measurements are conducted in the high- and low-power modes to provide data that is linear. The synthesizers are phase-locked to a master rubidium clock to ensure synchronization between transmitter and receiver. The equipment is securely and safely mounted on racks inside the van as shown in Fig. 5.

The 10-MHz IF signal is fed into the high-speed digitizer which samples the signal at a rate of 40 Mbps.

The digitizer contains four high-speed 14-bit analog-to-digital (ADC) converters, which digitize four 10-MHz IF channels simultaneously. Timing control is provided by an ITS-designed field programmable gate array (FPGA) and the ADC timing controller on the card. The card produces a 4-channel bit stream which is stored on a computer-controlled 300 GB redundant array of inexpensive disks (RAID).

V. Post Processing

The measurement system transmits a 511-bit PN as a BPSK RF signal. This signal propagates into the environment where it undergoes multiple reflections and diffractions, penetrates through structures, and ultimately reaches the receiver. The received signal is a superposition of PN sequences that have traveled over the various propagation paths. Fig. 6 shows a segment of the transmitted input PN sequence along with a segment of the digitized 10-MHz IF in which the distortion caused by propagation effects is visible.

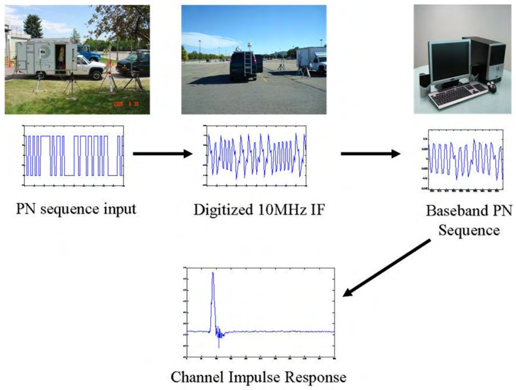

Fig. 6. Impulse response extraction process.

The digitized data are post-processed using an ITS-developed software program. The program converts the binary output of the digitizer into decimal format, and it separates the data from the four channels. Next, the program converts the digitized IF down to a baseband sequence with in-phase (I) and quadrature (Q) outputs.

A well-known property of a PN sequence is that it has an auto-correlation function that is an impulse function. We exploit this property to convert a PN sequence into the channel impulse response. The channel impulse response is generated by cross-correlating the received PN sequence with the input PN sequence. The result is a complex time series

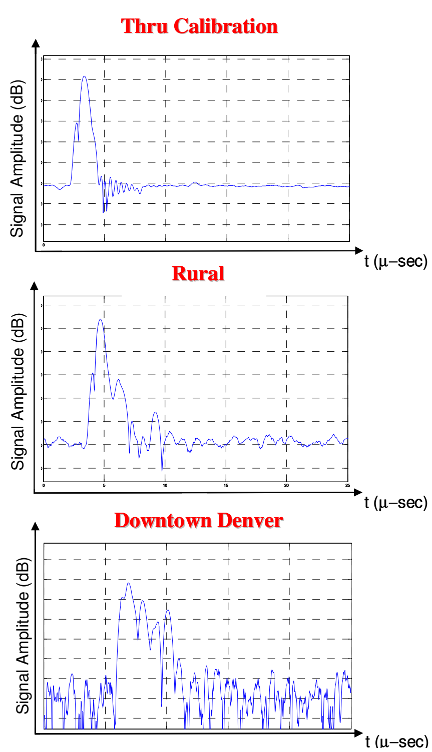

Fig. 7. 183-MHz channel impulse response magnitudes obtained under different conditions. (a) Thru calibration. (b) Rural. (c) Deep urban canyon. The time scale is 5 μ -sec per major division.

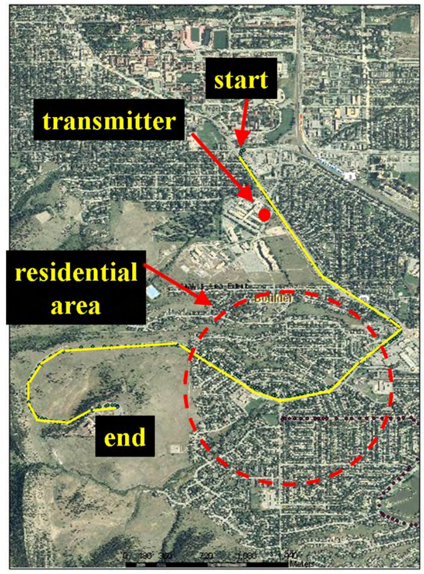

Fig. 8. Transmitter location and receiver van route

with both I- and Q-components. Fig. 7 shows the magnitude of the channel impulse response for selected 183-MHz measurement scenarios.

VI. Broadband Time-Domain Results

One useful way to present measured propagation data is to combine channel impulse responses from multiple locations on one graph. In this case we plot time as the abscissa and the impulse number as the ordinate. The strength (magnitude) of the impulse can be represented on a color scale on the graph.

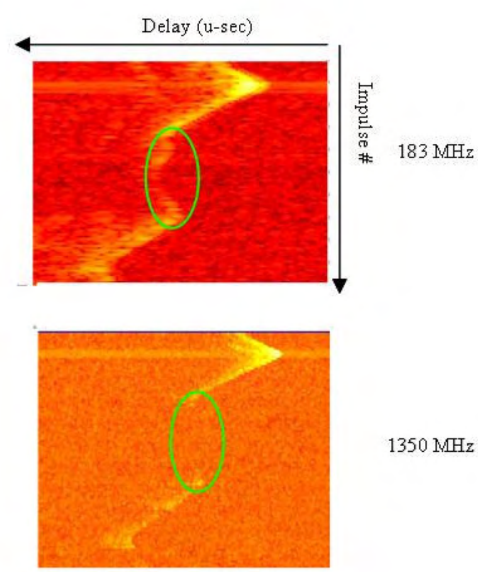

Fig. 9. 183- and 1350-MHz channel impulse response data obtained for the route of Fig. 8.

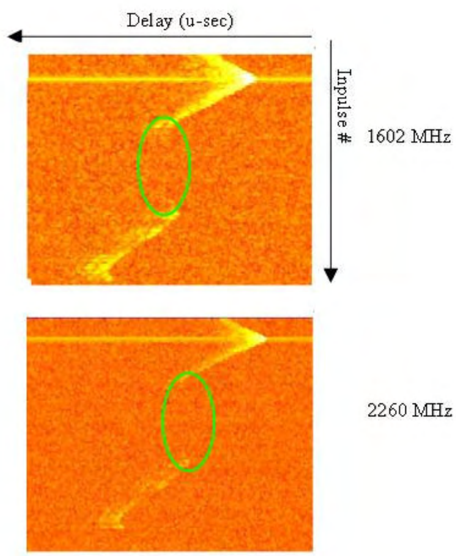

Fig. 10. 1602- and 2260-MHz channel impulse response data obtained for the route of Fig. 8.

The result is a two-dimensional graph that provides a lot of information about channel propagation effects along a given measurement route.

A series of system tests were performed in Boulder, Colorado in August, 2007. The transmit location and drive route are shown in Fig. 8. The transmitter truck was parked at the ITS Boulder Laboratories and the receiver van was driven south on Broadway to Table Mesa Drive. The van then travelled in a westerly direction until it reached the summit of Table Mesa. Figs. 9 through 11 depict combined impulse response results obtained from these tests.

Plots are provided for the 183-, 1350-, 1602-, 2260-, and 5750-MHz channels. The horizontal axis contains the time axis with a maximum value of 251 μsec for the 183-MHz band, 102 μsec for the 1602-MHz band, and 51 μsec for the 1350-, 2260-, and 5750-MHz bands. The vertical axis corresponds to an impulse response obtained at even 5-second intervals along the entire length of the drive. The resulting graph contains 100 channel impulse responses.

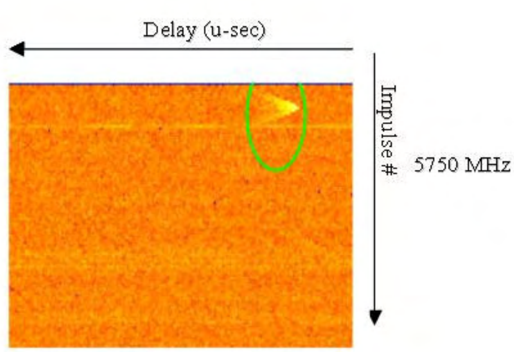

Fig. 11. The 5750 MHz channel impulse response data obtained for the route of Fig. 8.

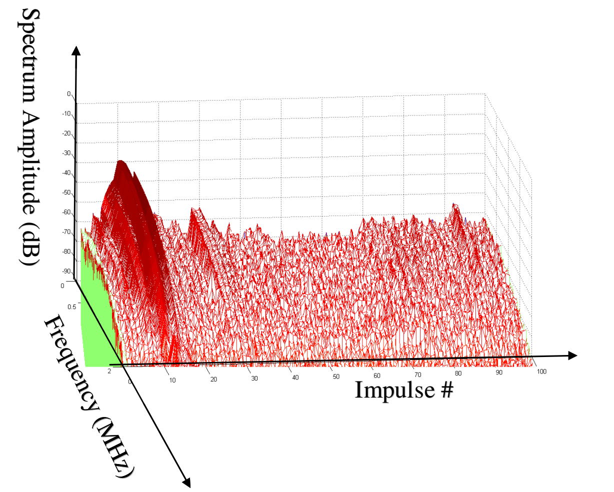

Fig. 12. Frequency-domain amplitude spectra obtained from the 183-MHz channel impulse responses.

The graphs show impulse response strengths as a function of position along the drive. With the transmitter truck configured in the high-power mode, the van begins receiving data at the intersection of Baseline Road and Broadway, and heads southeast. As the van approaches the transmitter, the impulse response grows larger, and the time delay decreases as well.

As the van passes close to the transmitter location, the peak impulse response levels are quite strong, resulting in receiver saturation. This can be seen as a horizontal flash in all of the graphs. After the van passes the transmitter, the time delay of the impulse increases and the signal level drops as the distance increases.

The van then turns onto Table Mesa Drive and heads southwest. Due to blockage effects from a combination of private homes and low-rise apartment buildings in a large residential area, the signal levels drop noticeably during this portion of the drive (annotated with a green ellipse in Figs. 9-11). The blockage effects become more pronounced at the

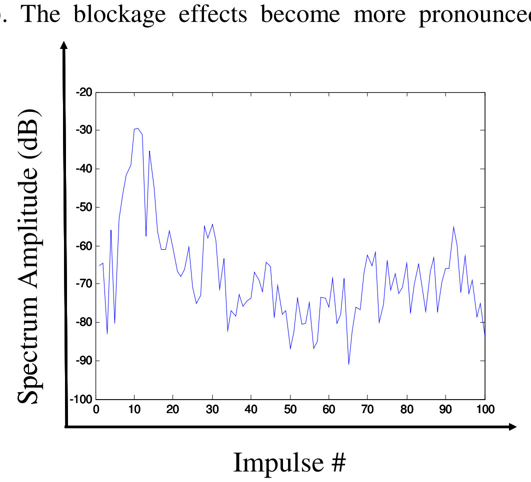

Fig. 13. Frequency-domain amplitude spectra as a function of burst number for a selected FFT bin. The data are sampled at 5-sec intervals.

higher frequencies. For instance, some signal is still visible at 183 MHz, while it disappears at 1350 MHz, 1602.5 MHz, and 2260 MHz.

After the van passes through the residential area and heads on a more westerly course, the signals on these four channels reappear for the duration of the drive. Conditions either approach line-of site or diffract over a nearby ridge. The 5750-MHz signal disappears completely after entering the residential area and does not reappear for the duration of the drive. The results indicate that, for these conditions, the lower frequencies propagate more effectively.

VII. Narrowband Time-Domain Results

The baseband channel impulse responses can be processed to yield narrowband frequency-domain magnitude and phase information. The process consists of applying a fast Fourier Transform (FFT) to the channel impulse responses.

The frequency resolution is the inverse of the duration of the channel impulse response. A 51-μsec impulse response duration yields a resolution of 19.6 kHz; a 102-μsec duration corresponds to a resolution of 9.8 kHz, and a 255-μsec duration yields a resolution of 3.9 kHz. These results can be used to examine narrowband fading effects.

Fig. 12 shows the frequency domain results for the 183-MHz channel. Amplitude spectrum results are plotted over the 2-MHz channel as a function of bandwidth and the burst number. The resulting three-dimensional plot is a composite of 100 FFTs (one FFT per impulse). Once again peak signal levels are observed at the point of closest approach as the van passes the ITS lab parking lot. The plot exhibits complex behavior with rapid variations with respect to both frequency and burst number. If we now select one frequency bin (3.9-kHz wide) and plot spectrum amplitude, we obtain the graph of Fig. 13. The samples are obtained at 5-second intervals, and the signal level profile is clearly visible. Complex multipath effects account for the rapid variation in signal levels.

VIII. Conclusions

The ITS mobile-to-mobile propagation measurement system has been deployed in a variety of urban and rural environments. The system has the ability to acquire large amounts of data on-the-fly, and a lot of propagation data has been obtained in both the time- and the frequency-domain. The results look promising and demonstrate the versatility and flexibility of this propagation measurement system.

Acknowledgment

We appreciate the generous support of our colleagues in the Office of Spectrum Management. In particular, we are indebted to Alaka Paul, Ed Drocella, Dave Anderson, and Karl Nebbia of OSM for excellent support, guidance and a high level of interest in our work. We also appreciate the generous level of support and guidance from Frank Sanders, Patti Raush, Randy Hoffmann, and Eric Nelson of the ITS management team.

References

[1] R.W. Hubbard, "Characteristics and applications of the PN channel probe," OT Technical Memorandum 76-218, 1976.

[2] K.C. Allen and W.A. Lindsey-Stewart, Method and apparatus for measuring the impulse response of a radio channel," U. S. Patent 5371760, Dec. 6, 1994.

[3] R.W. Hubbard, L.E. Pratt, and W.J. Hartman, "The measurement of microwave multipath in an airport environment," Department of Transportation Report FAA-RD-76-163, Jan. 1977. (NTIA sponsor report)

[4] R.W. Hubbard, R.F. Linfield, and W.J. Hartman, "Measuring characteristics of microwave mobile channels," NTIA Report 78-5, Jun. 1978.

[5] G.A. Hufford, R.W. Hubbard, L.E. Pratt, J.E. Adams, and S.J. Paulson, "Wideband propagation measurements in the presence of forests," U.S. Army Communications Electronics and Command Research and Development Technical Report CECOM 82-CS029-F, 1982. (NTIA sponsor report)

[6] J.A. Wepman, J.R. Hofmann, and L.H. Loew, "Impulse response measurements in the 1850-1990 MHz band in large outdoor cells," NTIA Report 94-309, Jun. 1994.

[7] P. Papazian and M. Cotton, "Relative propagation measurements between 430 MHz and 5750 MHz for mobile communication systems in urban environments," NTIA Report TR-04-407, Dec. 2003.

[8] P. Papazian and P. McKenna, "Short-range propagation measurements for interference model development," Proceedings of the International Symposium on Advanced Radio Technologies, pp. 94-99, NTIA Special Publication SP-07-445, Feb. 26-28, 2007.